

Low-dose irradiation inhibits proliferation of the *p53^{null}* type human prostate cancer cells through the ATM/p21 pathway

SI-JIE LI¹, XIN-YUE LIANG², HAI-JUN LI³, GUO-ZI YANG⁴, WEI LI², ZHUO LI⁵,
LEI ZHOU², XUE WEN², DE-HAI YU² and JIU-WEI CUI²

¹Department of Breast Surgery, ²Cancer Center, ³Institute of Translational Medicine, Departments of ⁴Radiation-Oncology, and ⁵Endocrinology and Metabolism, The First Hospital of Jilin University, Changchun, Jilin 130021, P.R. China

Received May 13, 2016; Accepted October 25, 2017

DOI: 10.3892/ijmm.2017.3237

Abstract. Low-dose ionizing radiation (LDIR) induces hormesis, exerts an adoptive effect on normal mammalian cells and stimulates cell proliferation; however, this effect is absent in cancer cells. Little is known on the molecular mechanisms underlying this differential response between normal and cancer cells. In the present study, it was demonstrated that the human prostate cancer cell line PC-3 and the normal prostate cell line RWPE-1 exhibited differential biological responses to LDIR. Through cell cycle analyses, it was demonstrated that LDIR inhibited cell growth and arrested the cell cycle at the S and G2/M phases in PC-3 cells, but not in RWPE-1 cells. Using western blotting, it was demonstrated that LDIR at 75 mGy induced the expression of ataxia-telangiectasia mutated (ATM) protein in PC-3 as well as RWPE-1 cells. However, the ATM/p21 pathway was activated in PC-3, but not in RWPE-1 cells. Although the expression of p53 was not affected by 75 mGy LDIR in RWPE-1 cells, the ATM/p21 pathway was activated when RWPE-1 cells lost p53 function. In addition, when using ATM inhibitors, the ATM/p21 pathway was inactivated in both cell lines, and the LDIR-induced cell proliferation inhibition was also abolished. These findings suggested that the ATM/p21 pathway directly participated in the LDIR-induced cell proliferation inhibition in *p53^{null}* type prostate tumor cells, whereas this mechanism was absent in normal prostate cells. Thus, p53 may affect cell stability following LDIR, and plays a crucial role in regulating the ATM/p21 pathway activated by LDIR.

Introduction

A low level of radiation exists extensively in our living and working environment, particularly in hospital-based radio-

therapy facilities, inevitably increasing the risk of constant exposure to low-dose ionizing radiation (LDIR). Unlike high-dose ionizing radiation (HDIR), LDIR has been proven to have different biological functions, such as hormesis (1,2) and the adoptive effect (3). Our previous studies indicated that LDIR stimulates the proliferation of normal cells, including rat mesenchymal stem cells, mouse bone marrow hematopoietic progenitor cells and several normal human cell lines, such as MRC-5, HL-7702, 293T and 6550 HLEPiC. However, it does not stimulate the proliferation of cancer cell lines, such as K562, HL-60, NCI-H446, BEL7402, U251, HCT-8 and HeLa (4-6). We also demonstrated that LDIR augments the expansion and cytotoxicity of cultured human natural killer cells *in vitro* (7).

Prostate cancer is the second most frequently diagnosed cancer in men worldwide (8). Radiation therapy is one of the most common methods for the treatment of prostate cancer in clinical practice, usually at doses >70 Gy (9). However, the biological effect of LDIR on prostate cancer is seldom investigated, even *in vitro*. Since it was demonstrated that cells exposed to LDIR may exhibit differential responses, it would be of interest to investigate the molecular changes in prostate cancer cells following LDIR.

Ataxia-telangiectasia mutated (ATM) is a crucial factor involved in the processing of DNA damage, maintenance of genome stability and control of cell cycle progression (10). According to Suzuki *et al*, phosphorylated ATM foci were detected immediately after normal human diploid cells were irradiated by LDIR (11). As a radiation sensor, the activation of ATM is proven to be an early event and will interact with several cell signaling pathways, such as Akt and mitogen-activated protein kinase kinase/extracellular signal-regulated kinase (ERK) (12,13).

p53 is a key factor in the process of radiation response, controlling the activation of DNA repair and cell apoptosis pathways following acute radiation injury (14,15). Furthermore, the *p53* gene is the most frequent target for mutation and deletion in human cancers, with over half of all tumors exhibiting p53 mutations (16). Therefore, investigating the behavior of *p53^{null}* prostate tumor cells and elucidating the role of p53 in normal prostate cells after LDIR, may prove valuable for the radiation treatment of prostate cancer.

Correspondence to: Dr De-hai Yu or Dr Jiu-wei Cui, Cancer Center, The First Hospital of Jilin University, 71 Xinmin Street, Changchun, Jilin, 130021, P.R. China
E-mail: yudehai@jlu.edu.cn
E-mail: cuijw@jlu.edu.cn

Key words: low-dose ionizing radiation, ataxia-telangiectasia mutated, p21, p53, prostate cancer

Materials and methods

Cell cultivation and treatments. The human prostate cancer cell line PC-3 and the normal prostate cell line RWPE-1 were purchased from American Type Culture Collection (Manassas, VA, USA). PC-3 was maintained in Dulbecco's modified Eagle's medium (DMEM; Life Technologies, Thermo Fisher Scientific, Shanghai, China) supplemented with 10% fetal bovine serum (HyClone, Beijing, China) and 1% antibiotics (penicillin-streptomycin; Invitrogen, Thermo Fisher Scientific, Carlsbad, CA, USA). RWPE-1 cells were maintained in Keratinocyte-Serum Free Media (KSFM; Life Technologies, Thermo Fisher Scientific, Grand Island, NY, USA) supplemented with 20 mg/ml bovine pituitary extract and 2 ng/ml epidermal growth factor (both from Invitrogen, Thermo Fisher Scientific). All cells were cultured at 37°C in a humidified incubator with a constant air flow of 5% CO₂.

In order to inhibit the function of p53 and ATM, 10 μ M pifithrin- α (PFT- α ; Beyotime Institute of Biotechnology, Haimen, China) dissolved in dimethyl sulfoxide and 5 mM caffeine (both from Sigma-Aldrich, Merck KGaA, Shanghai, China) dissolved in distilled water were added to the cell culture media 24 and 2 h prior to irradiation. Media containing the chemical inhibitors were replaced with fresh medium immediately after the irradiation.

Irradiation strategy. Monolayer cells were irradiated at a dose rate of 12.5 mGy/min by X-RAD 320 (Precision X-Ray, North Branford, CT, USA). The total dose was 20, 50, 75 or 100 mGy. After that, cell culture media were replaced and cells were harvested immediately or continually cultured until the next step experiment was performed. Control groups were treated similarly, except for the irradiation.

Cell proliferation assay. At 24 h prior to irradiation, 3×10^3 PC-3 and RWPE-1 cells were seeded in 96-well plates and then irradiated with 20, 50, 75 or 100 mGy of X-rays. After the irradiation, the cells were immediately transferred to the incubator and cultured for a further 12, 24, 48 or 72 h. Cell proliferation assays were determined using WST-1 Cell Proliferation reagent (Roche, Shanghai, China). According to the manufacturer's instructions, 20 μ l WST-1 were added to 200 μ l cell culture medium and then incubated in the dark for 2 h. Subsequently, the absorbance at 450 and 630 nm was measured by a microplate reader (Synergy HT; BioTek, Beijing, China). The final optical density (OD) was designated as OD₄₅₀-OD₆₃₀-OD_{blank}.

Cell cycle assay. Approximately 2×10^6 irradiated or sham-irradiated cells were collected and washed with 1 ml cold phosphate-buffered saline (PBS) twice to remove residual trypsin and serum. The cells were pelleted and resuspended in 1 ml fixation solution (300 μ l PBS and 700 μ l ethanol). Following incubation at 4°C for 4 h, the cells were centrifuged at 250 \times g for 5 min and the fixation solution was removed. After washing twice with 1 ml PBS, the cells were pelleted and suspended in 0.5 ml propidium iodide (PI; Sigma-Aldrich, Merck KGaA) staining solution (50 μ g/ml PI, 20 μ g/ml RNase A and 0.2% Triton X-100) and incubated in the dark at 37°C for 30 min. Cell suspensions were filtered through a 400-mesh sieve prior to being analyzed by a BD FACSCalibur flow cytometer (Becton-Dickinson, Sparks, MD, USA).

Protein extraction and western blot analysis. Cell total protein was extracted with RIPA buffer (Beyotime Institute of Biotechnology) supplemented with cocktail protease inhibitor (Roche), and the protein concentration was determined by bicinchoninic acid protein assay kit (Beyotime Institute of Biotechnology).

A total of 5-40 μ g cell total protein was separated by 4-8%, 5-10% or 5-15% sodium dodecyl sulfate-polyacrylamide gel electrophoresis (SDS-PAGE), and was then electrophoretically transferred to polyvinylidene difluoride membranes (0.45 μ m; Millipore, Billerica, MA, USA) and blocked at 37°C for 1 h with 5% skimmed milk in TBST [TBS (10 mmol/l Tris pH 7.5, 150 mmol/l NaCl) containing 0.1% Tween-20]. Subsequently, the membranes were incubated with the following antibodies: mouse monoclonal antibody against p53 (DO7; sc-47698, 1:1,500; Santa Cruz Biotechnology, Inc., Santa Cruz, CA, USA), rabbit monoclonal antibody against phospho-p53 (Ser15; D4S1H; cat. no. 12571, 1:1,000; Cell Signaling Technology, Danvers, MA, USA), rabbit polyclonal antibody against p21 (C-19; sc-397, 1:500; Santa Cruz Biotechnology, Inc.), rabbit monoclonal antibody against ATM (Y170; ab32420, 1:1,000; Abcam, Shanghai, China) and mouse monoclonal antibody against β -actin (C-2; sc-8432, 1:3,000; Santa Cruz Biotechnology, Inc.) at 4°C overnight. After washing for 3 \times 5 min with TBST, the membranes were incubated with horseradish peroxidase-conjugated goat anti-mouse (ZB-2305) or goat anti-rabbit (ZB-2301) secondary antibodies [IgG (H+L); 1:5,000; ZSGB-BIO, Beijing, China] at 37°C for 1 h. After washing for another 3 times, the immunocomplexes were detected with enhanced chemiluminescence (Thermo Fisher Scientific, Beijing, China) and X-ray film (Kodak, Beijing, China). Protein expression levels were determined semiquantitatively by densitometric analysis with the Quantity One software (Bio-Rad, Hercules, CA, USA).

Statistical analysis. All data and results were calculated from at least three replicate measurements and presented as means \pm standard deviation. The significance was determined by the Student's t-test using SPSS 20.0 software (IBM SPSS, Armonk, NY, USA). $P < 0.05$ was considered statistically significant ($P < 0.05$ and $P < 0.01$).

Results

LDIR induces differential cell growth in prostate cancer PC-3 and normal RWPE-1 cells. In order to investigate the effect of LDIR on prostate cancer PC-3 and normal RWPE-1 cells, four different doses of LDIR were delivered, namely 20, 50, 75 and 100 mGy. Cell proliferation was determined by WST-1 24 h post-LDIR. It was observed that LDIR doses of 50, 75 and 100 mGy significantly inhibited the growth of PC-3 cells compared with the sham-irradiated group ($P < 0.01$; Fig. 1A, left panel). Among these, the 75-mGy dose exerted the most prominent effect. By contrast, none of the radiation doses affected the growth of RWPE-1 cells ($P > 0.05$; Fig. 1A, right panel).

Cell growth in the two cell lines was compared at different timepoints following LDIR at 75 mGy. Cell proliferation was determined by WST-1 at 0, 12, 24, 48 and 72 h post-LDIR. PC-3 cells exhibited decelerated proliferation between 12 and 72 h after 75 mGy LDIR ($P < 0.05$ and $P < 0.01$, respectively) (Fig. 1B). However, normal prostate RWPE-1

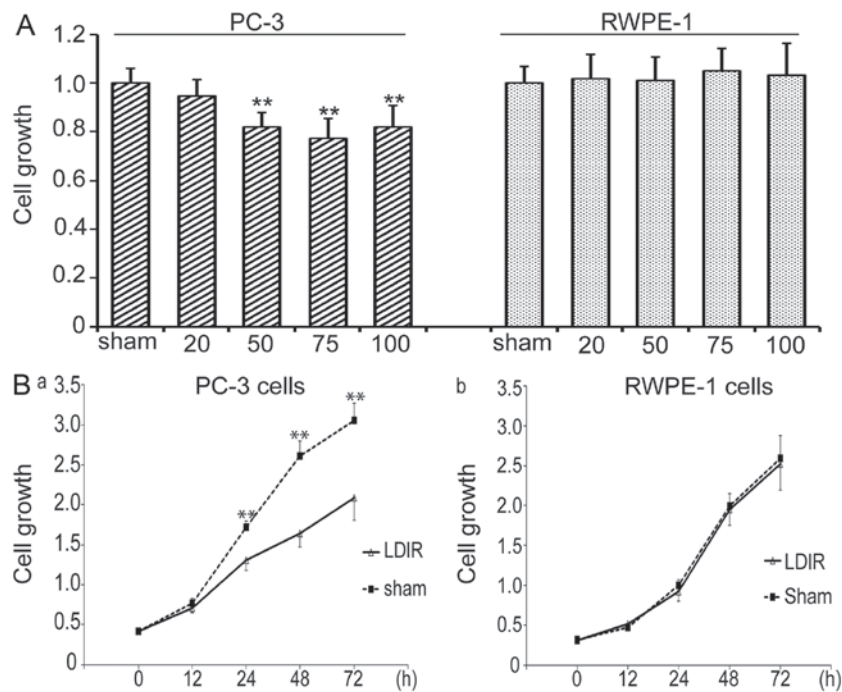


Figure 1. Low-dose ionizing radiation (LDIR) induces differential responses in PC-3 and RWPE-1 cells. (A) The cells were irradiated with 20, 50, 75 and 100 mGy LDIR, and cell growth was determined by WST-1 at 24 h post-LDIR. PC-3 cells exhibited decreased growth after 50, 75 and 100 mGy of LDIR, whereas 75 mGy exerted the most prominent inhibitory effect; however, none of the four doses of LDIR affected the growth of normal prostate RWPE-1 cells. ** $P < 0.01$. (B) The growth of PC-3 and RWPE-1 cells after 75 mGy LDIR was recorded, and cell proliferation was determined by WST-1 at 12, 24, 48 and 72 h post-LDIR. (a) PC-3 cells exhibited significantly decreased proliferation at 24, 48 and 72 h post-LDIR. (b) RWPE-1 cells exhibited no change in proliferation after 75 mGy LDIR. ** $P < 0.01$.

cells exhibited no obvious changes after 75-mGy irradiation compared with the sham control group ($P > 0.05$).

LDIR arrests the cell cycle at S and G2/M in PC-3 cells. Flow cytometry was then used to analyze cell cycle distribution at 24 h post-LDIR. It was observed that, after 75 mGy LDIR, PC-3 cells exhibited a significant S and G2/M phase arrest compared with the sham group (Fig. 2A). By contrast, there was no significant change in cell cycle distribution in RWPE-1 cells following LDIR (Fig. 2B). Quantitation data revealed that, in PC-3 cells, the S phase percentage increased 1.29-fold (36.7 vs. 28.4%, $P < 0.01$) and the G2/M phase percentage increased 1.69-fold (29 vs. 17.2%, $P < 0.01$; Fig. 2C).

LDIR does not affect p53. Of note, 75 mGy LDIR only inhibited the proliferation and cell cycle progression in PC-3 cells, but not in normal prostate cells. PC-3 is a *p53*^{null} cell line. Since p53 is the most significant radiation-related protein, the expression of p53 and phosphorylated p53 (Ser-15, p-p53) in RWPE-1 cells was first examined. However, the western blotting results revealed no significant changes in the expression of p53 or p-p53 at 2, 4 and 8 h after 75 mGy LDIR, compared with that of the sham-irradiation group (Fig. 3).

LDIR specifically activates the ATM/p21 pathway in p53-deficient cancer cells. The expression of ATM, which is also a well-known critical DNA damage and radiation response sensor in mammalian cells, was further examined (17). At 2, 4 and 8 h post-LDIR, the total proteins of PC-3 and RWPE-1 cells were extracted and separated by 4-8% SDS-PAGE, and the expression of ATM was detected by western blotting. The

expression of ATM was found to be upregulated by 75 mGy LDIR in PC-3 as well as RWPE-1 cells at 2 and 4 h post-LDIR (Fig. 4A and C, lanes 5 and 6). In PC-3 cells, the expression of ATM was upregulated 2.8- and 2.04-fold, respectively (Fig. 4B, left panel; $P < 0.05$). In RWPE-1 cells, the ATM was activated 2.08- and 1.4-fold (Fig. 4D, left panel). At 8 h post-LDIR, the expression of ATM in both cell lines recovered to a similar level as in the sham-irradiated group (Fig. 4A and C, lane 7).

The expression of p21 was also quantitated in PC-3 and RWPE-1 cells by western blot analysis after 75 mGy LDIR. In PC-3 cells, a significant upregulation of p21 was observed after LDIR (Fig. 4A, lanes 5-7 and B, right panel). However, the LDIR-induced p21 upregulation was absent in normal RWPE-1 cells (Fig. 4C, lanes 5-7 and D, right panel).

In order to mimic the p53 dysfunction in PC-3 cancer cells, 10 μ M PFT- α were used to inactivate p53 in normal RWPE-1 cells prior to 75 mGy LDIR, and the expression of ATM and p21 was measured by western blot analysis. Compared with the non-irradiated group, the expression of ATM was found to be significantly increased 2.13-, 2.14- and 1.8-fold at 2, 4 and 8 h post-LDIR, respectively (Fig. 4C, lanes 2-8 and 8-10 and D, left panel; $P < 0.05$). Of note, RWPE-1 cells exhibited a significant upregulation of p21 (1.74-, 1.88- and 1.55-fold at 2, 4 and 8 h post-LDIR, respectively) compared with cells that were only exposed to 75 mGy LDIR (Fig. 4C, lane 5-7 and 8-10 and D, right panel) ($P < 0.05$).

ATM inhibitors restore proliferation of PC-3 cells. To further investigate the role of the ATM/p21 pathway in LDIR-induced changes in cell proliferation, caffeine was used to block the function of ATM. Following inhibition of ATM with caffeine, the proliferation of PC-3 cells and PFT- α -treated RWPE-1 cells

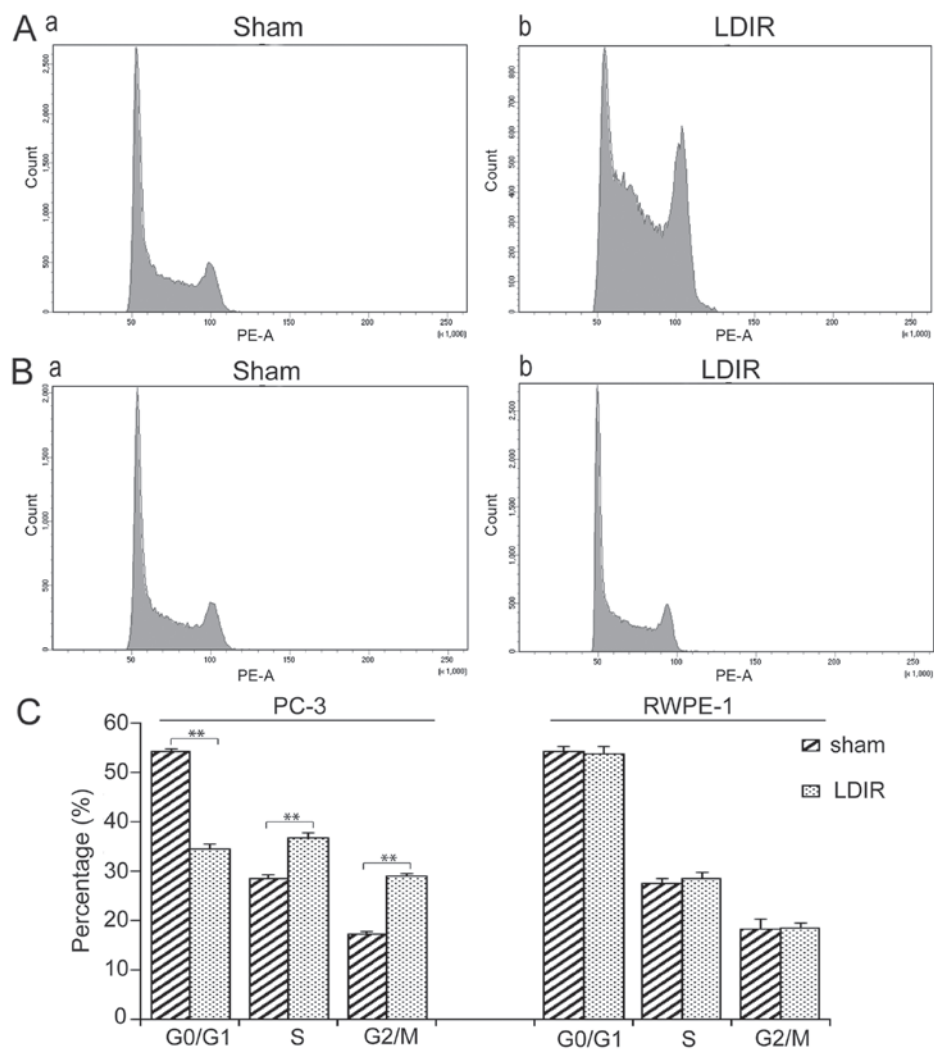


Figure 2. Low-dose ionizing radiation (LDIR) induces S and G2/M phase arrest in PC-3 cells. (A) Cell cycle distribution of PC-3 cells. Following LDIR, cell distribution was determined by flow cytometry at 24 h post-LDIR. (a) Sham-irradiated PC-3 cells; (b) 75 mGy-irradiated PC-3 cells. (B) Cell cycle distribution of RWPE-1 cells. (a) Sham-irradiated RWPE-1 cells; (b) 75 mGy-irradiated RWPE-1 cells. (C) Mean percentage of cells in each cell cycle phase. ** $P < 0.01$.

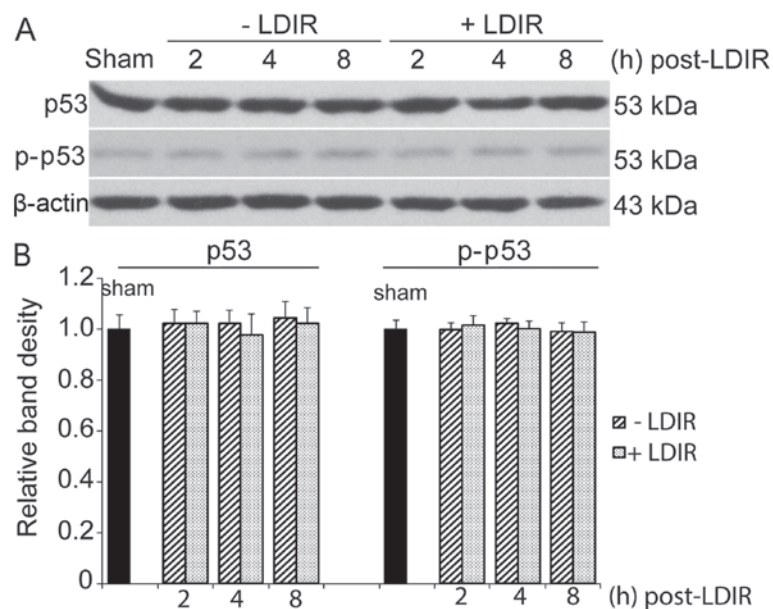


Figure 3. Low-dose ionizing radiation (LDIR) does not affect the expression of p53/p-p53 in RWPE-1 cells. (A) Western blotting. Cells were irradiated by 75 mGy LDIR and total protein was extracted at 2, 4 and 8 h post-LDIR. The expression of p53 and p-p53 was determined by western blotting. Representative blots of 3 experiments are shown. (B) Quantification of blots via measuring the relative band density.

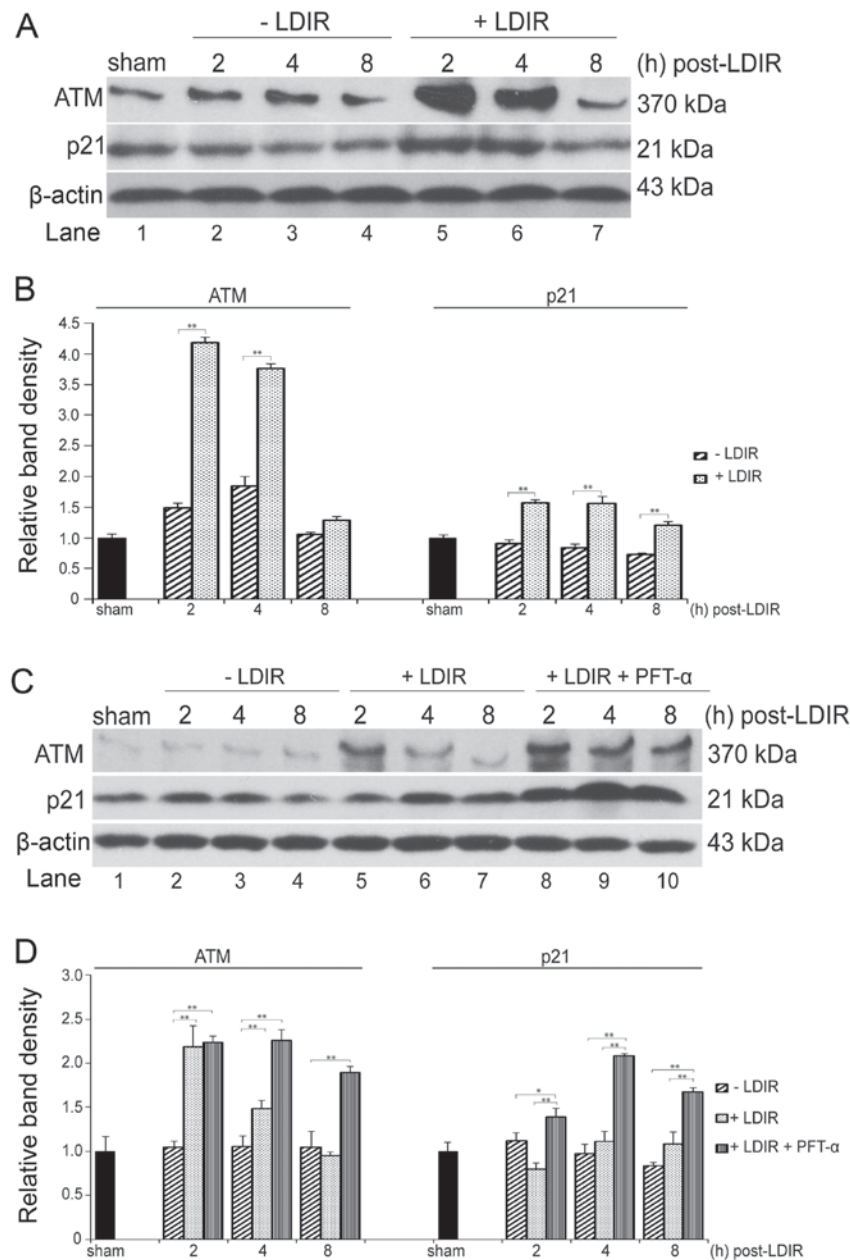


Figure 4. Low-dose ionizing radiation (LDIR) activates the ataxia-telangiectasia mutated (ATM)-p21 pathway in PC-3 cells. (A) ATM/p21 pathway in PC-3 cells. PC-3 cells were irradiated by 75 mGy LDIR and total protein was extracted at 2, 4 and 8 h post-LDIR. The activity of ATM and p21 was determined by western blotting. Representative blots of 3 experiments are shown. (B) Quantification of blots via measuring the relative band density of ATM and p21 in PC-3 cells. **P<0.01. (C) ATM/p21 pathway in RWPE-1 cells. Normal RWPE-1 cells and p53-inactivated RWPE-1 cells were irradiated with 75 mGy LDIR and total protein was extracted at 2, 4 and 8 h post-LDIR. The activity of ATM and p21 was determined by western blotting. Representative blots of 3 experiments are shown. (D) Quantification of blots via measuring the relative band density of ATM and p21 in RWPE-1 cells. **P<0.01. PFT- α , pifithrin- α .

was measured at 24 h post-LDIR. We found that, after caffeine treatment, the proliferation inhibition in PC-3 cells as well as in p53-inactivated RWPE-1 cells was abolished (P<0.05; Fig. 5A), and the expression of p21 was restored to a level similar to that in the sham irradiation group (Fig. 5B and C). Taken together, these data suggest the involvement of the ATM/p21 pathway in the differential LDIR-induced biological effect in normal and p53^{null} prostate cancer cells (Fig. 5D).

Discussion

Different doses of radiation may exert distinct biological effects on normal and cancer cells. HDIR induces cell cycle arrest and

cell apoptosis, and it is commonly utilized in clinical practice for killing tumor cells. However, LDIR has a different biological function compared with HDIR. Doses of 75 and 50 mGy are the LDIR doses most frequently used in our laboratory to demonstrate the proliferation characteristics of several normal and tumor cell lines (5,6,18). The majority of these tested normal cell lines exhibit increased cell proliferation and S phase cell population, while this response is not observed in cancer cell lines. However, as is well-known, tumor cells are heterogeneous, and commonly harbor gene mutations. Therefore, determination of the differential LDIR response among diverse types of tumor cells may be of interest, and may be proven useful for individualizing radiotherapy. Since p53 gene mutations or deletions are

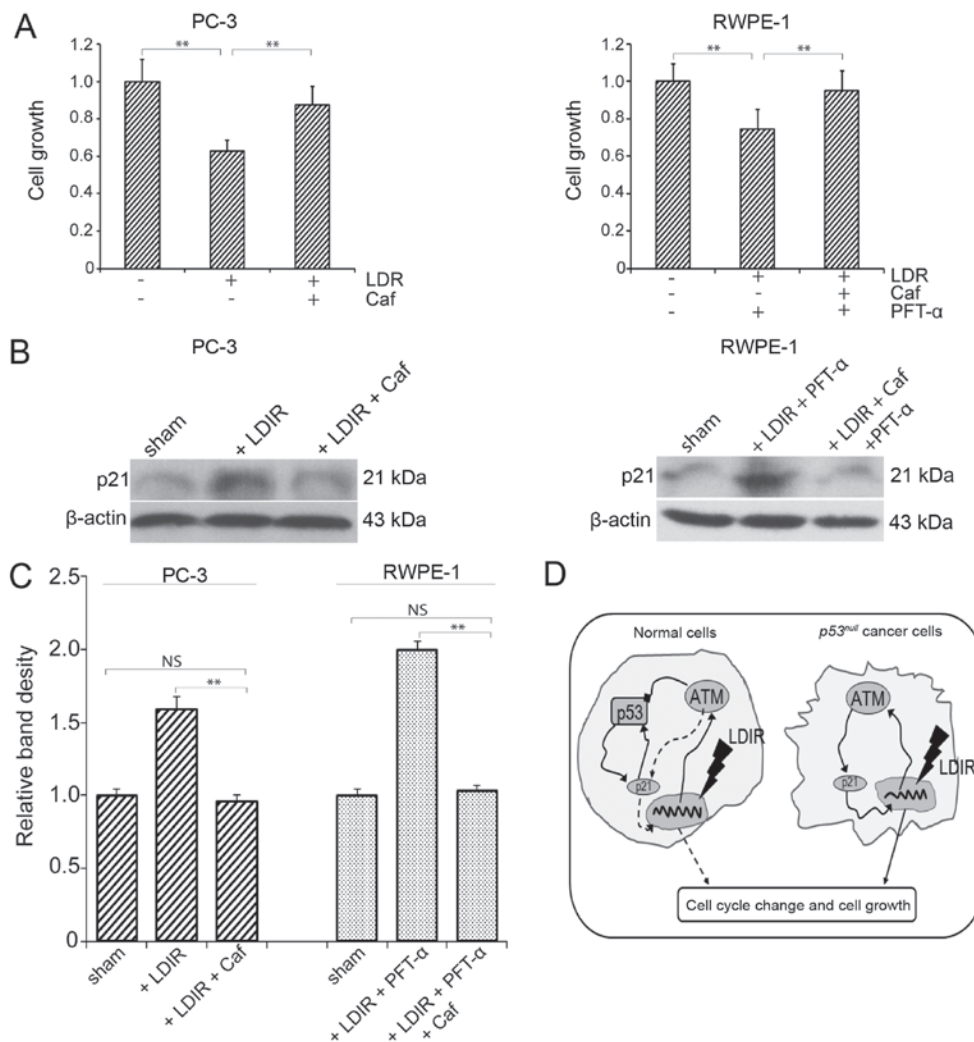


Figure 5. Ataxia-telangiectasia mutated (ATM) inhibitor abolishes the low-dose ionizing radiation (LDIR)-induced proliferation inhibition in PC-3 cells. (A) Cell growth following treatment with inhibitors. PC-3 cells as well as p53-inactivated RWPE-1 cells were treated with 5 mM caffeine (Caf) 2 h prior to irradiation by 75 mGy LDIR. Cell growth was determined by WST-1 at 24 h post-LDIR. (a) Caffeine, an ATM inhibitor, abolished the LDIR-induced proliferation inhibition in PC-3 cells. (b) Caffeine also abolished the LDIR-induced proliferation inhibition in p53-inactivated RWPE-1 cells. (B) p21 expression following treatment with inhibitors. PC-3 and RWPE-1 cells were treated as described above. The activity of p21 was determined by western blotting at 4 h post-LDIR. Representative blots of 3 experiments are shown. (C) Quantification of blots via measuring the relative band density of p21. ** $P < 0.01$; NS, not significant. (D) Putative mechanism underlying the differential biological effect following LDIR in normal RWPE-1 cells and prostate cancer cells. PFT- α , pifithrin- α .

common in tumor cells, in the present study a $p53^{null}$ type prostate tumor cell line (PC-3) and a normal prostate cell line (RWPE-1) were selected as the investigation model. First, changes in cell proliferation after LDIR were investigated. PC-3 cells exhibited radiation sensitivity to 20-100 mGy LDIR at a dose rate of 12.5 mGy/min, but RWPE-1 cells did not respond to this dose. This is the first time it was demonstrated that 75 mGy LDIR inhibits tumor cell proliferation in our laboratory. It remains unknown whether this is a general characteristic for all $p53^{null}$ type tumor cells, and more cell types must be investigated for confirmation.

The molecular mechanisms leading to different biological responses between normal and cancer cells are of particular interest. ATM acts upstream of several signal transduction pathways initiated by ionizing radiation, such as the Akt (12), ERK (13) and p53 pathways (19). Xie *et al* recently demonstrated that infiltrating mast cells may alter the sensitivity of prostate cancer to chemotherapy and radiotherapy via modulating p38/p53/p21 signaling and ATM phosphorylation (20).

Huang *et al* reported that extremely low-frequency electromagnetic fields inhibit HaCat cell proliferation and lead to a G1 phase arrest through the activation of the ATM-Chk2-p21 pathway (21). In the present study, we also demonstrated an intrinsic correlation between the LDIR-activated ATM-p53-p21 pathway and inhibition of cell proliferation. We found that, although 75 mGy LDIR activated ATM in $p53^{null}$ type PC-3 cells as well as in normal RWPE-1 cells, it only activated p21 and inhibited cell proliferation in PC-3 cells. We hypothesized that p53 blocks LDIR-induced cell signaling, as p53 acts as a DNA damage repairer and cell cycle arrestor (22). Therefore, the expression of p53 and p-p53 was investigated in RWPE-1 cells. No change in p53 and p-p53 expression was observed in RWPE-1 cells at 2, 4 and 8 h post-LDIR. However, the possibility that p53 is not involved in this process could not be excluded. Using inhibitors to inactivate p53 in RWPE-1 cells, we observed that LDIR induced p21 upregulation and cell proliferation inhibition, although the ATM upregulation remained unchanged. This is in consistent

with the findings in PC-3 cells. When the function of ATM was blocked, the LDIR-induced p21 overexpression and cell proliferation inhibition were abolished in both PC-3 and RWPE-1 cells.

p21 is a transcriptional target of p53, which induces cell cycle arrest through its function as a cyclin-dependent kinase inhibitor (23,24). However, in our LDIR model, following p53 inactivation, the expression of p21 increased significantly. Therefore, we hypothesized that there is a p53-independent ATM/p21 pathway in *p53^{null}* prostate cancer cells, which may be activated by LDIR and directly lead to cell cycle arrest and proliferation inhibition (Fig. 5D, right model). By contrast, in normal cells with wild-type p53, the classical ATM-p53-p21 pathway is a dominant irradiation response pathway (25). The difference in our model was that the radiation dose was insufficient for stimulating overexpression and phosphorylation of p53. However, although the p53/p-p53 ratio did not change, they play a key role in the feedback regulation of p21 (26), as well as the maintenance of the stability of mitosis. After p53 is blocked in normal cells, the ATM/p21 pathway may be activated by LDIR, to a similar extent as in PC-3 cells (Fig. 5D, left model). The effect of HDIR on the ATM/p21 pathway was also investigated. When the irradiation dose was increased to 2 Gy or higher, the expression of p53 in RWPE-1 cells markedly increased (data not shown). Unlike the interaction between ATM and p21 in LDIR, when cells were exposed to HDIR, the classical ATM, p53 and p21 crosstalk was proven to be the dominant response pathway when cells were exposed to HDIR, as previously reported (25,27). Of note, it remains unknown whether ATM directly activates p21 in this LDIR model, or whether there are other intermediate factors, such as Chk2 (21,28); further investigation is required to address this issue.

Acknowledgements

This study was supported by grants from the National Science Foundation of China (no. 81302380 to D.-H.Y. and no. 81302379 to X.-Y.L.) and the Jilin Provincial Science and Technology Department (no. 20140520017JH).

References

1. Luckey TD: Physiological benefits from low levels of ionizing radiation. *Health Phys* 43: 771-789, 1982.
2. Feinendegen LE: Evidence for beneficial low level radiation effects and radiation hormesis. *Br J Radiol* 78: 3-7, 2005.
3. Olivieri G, Bodycote J and Wolff S: Adaptive response of human lymphocytes to low concentrations of radioactive thymidine. *Science* 223: 594-597, 1984.
4. Li W, Wang G, Cui J, Xue L and Cai L: Low-dose radiation (LDR) induces hematopoietic hormesis: LDR-induced mobilization of hematopoietic progenitor cells into peripheral blood circulation. *Exp Hematol* 32: 1088-1096, 2004.
5. Liang X, So YH, Cui J, Ma K, Xu X, Zhao Y, Cai L and Li W: The low-dose ionizing radiation stimulates cell proliferation via activation of the MAPK/ERK pathway in rat cultured mesenchymal stem cells. *J Radiat Res (Tokyo)* 52: 380-386, 2011.
6. Jiang H, Xu Y, Li W, Ma K, Cai L and Wang G: Low-dose radiation does not induce proliferation in tumor cells in vitro and in vivo. *Radiat Res* 170: 477-487, 2008.
7. Yang G, Kong G, Wang G, Jin H, Zhou L, Yu D, Niu C, Han W, Li W and Cui J: Low-dose ionizing radiation induces direct activation of natural killer cells and provides a novel approach for adoptive cellular immunotherapy. *Cancer Biother Radiopharm* 29: 428-434, 2014.
8. Torre LA, Bray F, Siegel RL, Ferlay J, Lortet-Tieulent J and Jemal A: Global cancer statistics, 2012. *CA Cancer J Clin* 65: 87-108, 2015.
9. Cho E, Mostaghel EA, Russell KJ, Liao JJ, Konodi MA, Kurland BF, Marck BT, Matsumoto AM, Dalkin BL and Montgomery RB: External beam radiation therapy and abiraterone in men with localized prostate cancer: Safety and effect on tissue androgens. *Int J Radiat Oncol Biol Phys* 92: 236-243, 2015.
10. Savitsky K, Sfez S, Tagle DA, Ziv Y, Sartiel A, Collins FS, Shiloh Y and Rotman G: The complete sequence of the coding region of the ATM gene reveals similarity to cell cycle regulators in different species. *Hum Mol Genet* 4: 2025-2032, 1995.
11. Suzuki K, Okada H, Yamauchi M, Oka Y, Kodama S and Watanabe M: Qualitative and quantitative analysis of phosphorylated ATM foci induced by low-dose ionizing radiation. *Radiat Res* 165: 499-504, 2006.
12. Viniegra JG, Martínez N, Modirassari P, Hernández Losa J, Parada Cobo C, Sánchez-Arévalo Lobo VJ, Aceves Luquero CI, Alvarez-Vallina L, Ramón y Cajal S, Rojas JM, *et al*: Full activation of PKB/Akt in response to insulin or ionizing radiation is mediated through ATM. *J Biol Chem* 280: 4029-4036, 2005.
13. Ahmed KM, Nantajit D, Fan M, Murley JS, Grdina DJ and Li JJ: Coactivation of ATM/ERK/NF-kappaB in the low-dose radiation-induced radioadaptive response in human skin keratinocytes. *Free Radic Biol Med* 46: 1543-1550, 2009.
14. Lee CL, Blum JM and Kirsch DG: Role of p53 in regulating tissue response to radiation by mechanisms independent of apoptosis. *Transl Cancer Res* 2: 412-421, 2013.
15. Menon V and Povirk L: Involvement of p53 in the repair of DNA double strand breaks: Multifaceted Roles of p53 in homologous recombination repair (HRR) and non-homologous end joining (NHEJ). *Subcell Biochem* 85: 321-336, 2014.
16. Freed-Pastor WA and Prives C: Mutant p53: One name, many proteins. *Genes Dev* 26: 1268-1286, 2012.
17. Kim GD, Choi YH, Dimtchev A, Jeong SJ, Dritschilo A and Jung M: Sensing of ionizing radiation-induced DNA damage by ATM through interaction with histone deacetylase. *J Biol Chem* 274: 31127-31130, 1999.
18. Jiang H, Li W, Li X, Cai L and Wang G: Low-dose radiation induces adaptive response in normal cells, but not in tumor cells: In vitro and in vivo studies. *J Radiat Res (Tokyo)* 49: 219-230, 2008.
19. Canman CE, Lim DS, Cimprich KA, Taya Y, Tamai K, Sakaguchi K, Appella E, Kastan MB and Siliciano JD: Activation of the ATM kinase by ionizing radiation and phosphorylation of p53. *Science* 281: 1677-1679, 1998.
20. Xie H, Li C, Dang Q, Chang LS and Li L: Infiltrating mast cells increase prostate cancer chemotherapy and radiotherapy resistances via modulation of p38/p53/p21 and ATM signals. *Oncotarget* 7: 1341-1353, 2016.
21. Huang CY, Chang CW, Chen CR, Chuang CY, Chiang CS, Shu WY, Fan TC and Hsu IC: Extremely low-frequency electromagnetic fields cause G1 phase arrest through the activation of the ATM-Chk2-p21 pathway. *PLoS One* 9: e104732, 2014.
22. Roos WP, Thomas AD and Kaina B: DNA damage and the balance between survival and death in cancer biology. *Nat Rev Cancer* 16: 20-33, 2016.
23. Lin K, Adamson J, Johnson GG, Carter A, Oates M, Wade R, Richards S, Gonzalez D, Matutes E, Dearden C, *et al*: Functional analysis of the ATM-p53-p21 pathway in the LRF CLL4 trial: blockade at the level of p21 is associated with short response duration. *Clin Cancer Res* 18: 4191-4200, 2012.
24. Dotto GP: p21(WAF1/Cip1): More than a break to the cell cycle? *Biochim Biophys Acta* 1471: M43-M56, 2000.
25. Cao L, Kawai H, Sasatani M, Iizuka D, Masuda Y, Inaba T, Suzuki K, Ootsuyama A, Umata T, Kamiya K, *et al*: A novel ATM/TP53/p21-mediated checkpoint only activated by chronic γ -irradiation. *PLoS One* 9: e104279, 2014.
26. Pang LY, Scott M, Hayward RL, Mohammed H, Whitelaw CB, Smith GC and Hupp TR: p21(WAF1) is component of a positive feedback loop that maintains the p53 transcriptional program. *Cell Cycle* 10: 932-950, 2011.
27. Luo JL, Cao JP, Zhu W, Feng S, Sheng FJ, Zhu CY, Zheng SY: Interaction between ATM and radiation-activated phosphorylation of P53 and P21. *Ai Zheng* 24: 1059-1063, 2005 (In Chinese).
28. Aliouat-Denis CM, Dendouga N, Van den Wyngaert I, Goehlmann H, Steller U, van de Weyer I, Van Slycken N, Andries L, Kass S, Luyten W, *et al*: p53-independent regulation of p21Waf1/Cip1 expression and senescence by Chk2. *Mol Cancer Res* 3: 627-634, 2005.